Optics Letters

Scalable electro-optic frequency comb generation via dual-frequency-driven cascaded thin-film lithium niobate modulators

Zehong Wang,[1,2] Shuaishuai Liu,[1,2,*] Zhenguo Lu,[1,2] Xiaoyu Yang,[1,2] and Yongmin Li[1,2,3,4]

[1]State Key Laboratory of Quantum Optics Technologies and Devices, Institute of Opto-Electronics, Shanxi University, Taiyuan 030006, China
[2]Collaborative Innovation Center of Extreme Optics, Shanxi University, Taiyuan 030006, China
[3]Hefei National Laboratory, Hefei 230088, China
[4]yongmin@sxu.edu.cn
*liushuaishuai@sxu.edu.cn

Received 17 April 2026; revised 28 May 2026; accepted 22 June 2026; posted 22 June 2026; published 13 July 2026

Electro-optic frequency comb (EOFC), featuring high performance, flexibility, and on-chip integrability, has become a key technology for optical communications and precision metrology. In this work, we propose and experimentally demonstrate an efficient EOFC generation scheme on a thin-film lithium niobate (TFLN) platform. By driving cascaded TFLN modulators with two radio frequency (RF) signals at different frequencies and optimizing the driving parameters, we are able to generate an EOFC with a line spacing of 2.5 GHz and 432 comb lines with a flatness of 10 dB. The presented scheme substantially increases the number of comb lines compared to single-tone driving. The proposed approach offers an effective route to overcome the line-number scaling limit of conventional EOFCs, providing a practical path towards high-performance comb sources. © 2026 Optica Publishing Group. All rights, including for text and data mining (TDM), Artificial Intelligence (AI) training, and similar technologies, are reserved.

https://doi.org/10.1364/OL.601863

Introduction. Optical frequency combs (OFCs), characterized by uniform frequency spacing and coherent phase stability [1], have been widely employed in applications such as optical atomic clocks [2], absolute distance measurement [3], precision spectroscopy [4], and optical communications [5]. In optical atomic clocks, OFCs enable a direct link between optical and microwave frequencies, providing an unprecedented tool for pushing the accuracy of atomic clocks to their limits and underpinning modern science and technology [2]. In the field of absolute distance measurement, dual-comb ranging based on integrated microcavity coherent soliton pairs achieves nanometer-level precision, enabling applications ranging from surface profilometry and strain sensing to satellite formation [3]. Meanwhile, in precision spectroscopy, OFCs enable high-resolution molecular spectroscopy by mapping absorption and dispersion information into the radio-frequency domain via coherent heterodyne detection, achieving high-precision spectral reconstruction with measurement deviations below 1% without the need for active stabilization [4]. Additionally, in optical communication systems, each comb line can serve as an independent communication channel, enabling multi-channel parallel high-speed data communications through wavelength-division multiplexing, thereby significantly enhancing the channel capacity [5].

Currently, the main approaches for OFC generation include mode-locked lasers [6], microresonator Kerr frequency combs [7], and electro-optic modulation [8–10]. Mode-locked lasers are capable of generating OFCs with high power and repetition rates, but the tunability of the repetition rate is limited by the cavity length [6]. Microresonator Kerr frequency combs offer advantages such as compact footprint and low power consumption, and their ultra-broad spectra hold the potential to surpass the capacity limits of optical communications [7]; however, the line spacing is determined by the physical dimensions of the microcavity. Electro-optic frequency combs (EOFCs) are generated by driving electro-optic modulators with radio frequency (RF) signals to produce sidebands via intensity and phase modulation of a continuous-wave laser. They offer several advantages, including continuously tunable central wavelength and line spacing, controllable phase noise, high system stability, and ease of integration [8].

EOFCs based on bulk lithium niobate modulators are typically limited by the large half-wave voltage, resulting in a relatively small number of comb lines [11–13], which restricts their applicability in high-speed communications and precision measurements. For instance, the scheme proposed in [12] generated an EOFC with seven comb lines and a flatness of 1 dB. Although the flatness is good, the limited number of comb lines fails to meet the requirements of most EOFC applications. The scheme in [9] employed a phase modulator (PM) within a Sagnac interferometer, achieving 21 comb lines and a flatness of 7.8 dB, which similarly falls short for most application scenarios.

The emergence of thin-film lithium niobate (TFLN) modulators has enabled a significant extension in the number of comb lines, due to its low half-wave voltage [14,15]. However, most existing approaches aimed at increasing the number of comb lines rely on cascading of PMs. This approach

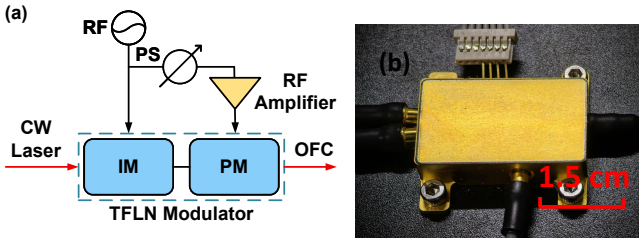

Fig. 1. (a) Schematic diagram of OFC generation using a single-frequency driven cascaded TFLN modulator: CW laser, continuous-wave laser; IM, intensity modulator; PM, phase modulator; PS, phase shifter; RF, radio frequency source; TFLN modulator, thin-film lithium niobate modulator. (b) Photograph of the TFLN modulator.

requires more modulators and increases power consumption. For example, the scheme proposed in [14] generated an EOFC with 148 comb lines and a flatness of 10 dB. While this approach achieves a significant increase in the number of comb lines, it requires one intensity modulator (IM) cascaded with three PMs. The increased components and power consumption limit its scalability.

To further address the challenge of the limited number of comb lines in EOFCs, this paper proposes an efficient generation scheme based on dual-frequency-driven cascaded TFLN modulators. Driving the cascaded TFLN modulators with two RF signals at different frequencies significantly increases the number of comb lines. We derive the principle of comb line multiplication and verify through simulations and experiments that, under the proposed dual-frequency driving scheme, the number of comb lines scales linearly with the frequency multiple of the drive signals. An EOFC generated using this scheme yields 432 comb lines within a 10 dB power variation. Compared to conventional cascaded electro-optic modulator schemes, this approach achieves a substantial increase in the number of comb lines. The proposed scheme is applicable to generating EOFCs with various line spacings within the bandwidth of the electro-optic modulators, offering a practical route toward large-scale comb line generation.

Theory. Figure 1(a) illustrates a typical scheme for generating an OFC using a single-frequency-driven cascaded TFLN modulators, which comprises of an IM and a PM [15]. Figure 1(b) shows the photograph of the TFLN modulator used in our experiment. The output optical field after the TFLN modulator is given by

$$E_{out}(t) = E\cos\left(\frac{\pi}{2V_{\pi_1}}(V_{DC}+V_I\cos\omega t)\right)\exp\left(i\frac{\pi V_P}{V_{\pi_2}}\cos\omega t\right)$$
$$= E\cos\left(\Gamma_B+\Gamma_m\cos\omega t\right)\exp\left(i\beta\cos\omega t\right), \quad (1)$$

where E is the amplitude of the input optical field, V_{π_1} is the half-wave voltage of the IM, V_{DC} and V_I are the bias voltage and the RF voltage applied to the IM, respectively, V_P is the RF voltage applied to the PM, V_{π_2} is the half-wave voltage of the PM, ω is the angular frequency of the RF signal, $\Gamma_B = (\pi V_{DC})/(2V_{\pi_1})$, $\Gamma_m = (\pi V_I)/(2V_{\pi_1})$, and $\beta = (\pi V_P)/(V_{\pi_2})$. From Eq. (1), the performance of the OFC depends on Γ_B, Γ_m, and β. As the modulation depth of the PM β increases, the number of comb lines in the OFC increases linearly [16]. In Fig. 2, we simulated the effects of the IM bias voltage and RF voltage on the flatness of the OFC and obtained the distribution of the

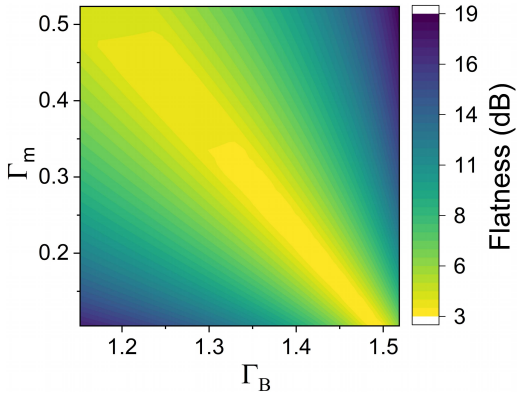

Fig. 2. Simulated flatness of the OFC as a function of different Γ_B and Γ_m.

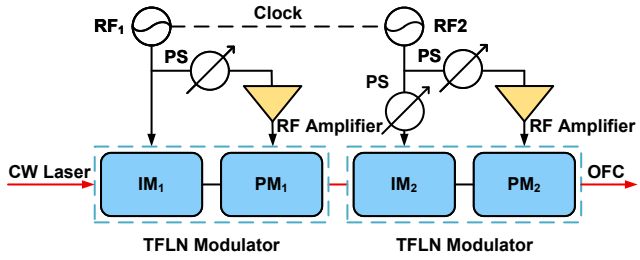

Fig. 3. Schematic diagram of OFC generation using a dual-frequency driven cascaded TFLN modulators. The dashed line between RF_1 and RF_2 indicates that the two RF sources are clock-synchronized.

OFC flatness. The color bar on the right indicates the flatness of the OFC in units of dB, where yellow represents good flatness, and purple represents poor flatness. Figure 2 indicates that the flatness is influenced by the synergistic variation of the two parameters, and the optimal flatness is achieved when $\Gamma_B = 1.44$ and $\Gamma_m = 0.20$.

To increase the number of OFC comb lines, we propose to drive cascaded TFLN modulators with two RF signals at different frequencies, as shown in Fig. 3. The output optical field after the cascaded TFLN modulators is given by

$$E_{\text{out}}(t) = E\cos(\Gamma_{B_1}+\Gamma_{m_1}\cos\omega_1 t)\cos(\Gamma_{B_2}+\Gamma_{m_2}\cos\omega_2 t)$$
$$\times\exp(i\beta_1\cos\omega_1 t)\exp(i\beta_2\cos\omega_2 t), \quad (2)$$

where ω_1 and ω_2 represent the angular frequencies of the RF signals driving the cascaded modulators, respectively. β_1 and β_2 represent the modulation depths of the two PMs. By applying the Bessel function, Eq. (2) can be simplified as

$$E_{\text{out}}(t) = \frac{E}{4}\sum_{n_1=-\infty}^{\infty}\sum_{n_2=-\infty}^{\infty}\sum_{n_3=-\infty}^{\infty}\sum_{n_4=-\infty}^{\infty} i^{n_3+n_4}$$
$$\times J_{n_1}(\Gamma_{m_1})J_{n_2}(\Gamma_{m_2})J_{n_3}(\beta_1)J_{n_4}(\beta_2)A_1A_2,$$
$$A_1 = \left[\exp\left(i\left[(n_1+n_3)\omega_1 t+\frac{\pi}{2}n_1+\Gamma_{B_1}\right]\right)\right.$$
$$\left.+\exp\left(-i\left[(n_1-n_3)\omega_1 t+\frac{\pi}{2}n_1+\Gamma_{B_1}\right]\right)\right],$$
$$A_2 = \left[\exp\left(i\left[(n_2+n_4)\omega_2 t+\frac{\pi}{2}n_2+\Gamma_{B_2}\right]\right)\right.$$
$$\left.+\exp\left(-i\left[(n_2-n_4)\omega_2 t+\frac{\pi}{2}n_2+\Gamma_{B_2}\right]\right)\right], \quad (3)$$

where J_n is the Bessel function of the first kind of order n. By applying the discrete Fourier transform, the expression of Eq. (3) in the frequency domain can be written as

$$E_{\text{out}}(\omega_k) = \frac{E}{4N}\sum_{n=0}^{N-1}\sum_{n_1=-\infty}^{\infty}\sum_{n_2=-\infty}^{\infty}\sum_{n_3=-\infty}^{\infty}\sum_{n_4=-\infty}^{\infty} i^{n_3+n_4} \times J_{n_1}(\Gamma_{m_1})J_{n_2}(\Gamma_{m_2})J_{n_3}(\beta_1)J_{n_4}(\beta_2)\,A_1\,A_2 \times \exp(-i\omega_k t_n), \quad k = 0, 1, \ldots, N-1. \tag{4}$$

The first cascaded TFLN modulators produce OFC with a comb line spacing of f_1. The second TFLN modulator performs further modulation on the OFC generated by the first TFLN modulator, producing comb lines with a spacing of f_2 for each original comb line. Since $f_1 > f_2$, the finer-spaced comb lines with spacing f_2 fill in the gaps between the original comb lines with spacing f_1, thereby achieving a multiplication in the number of comb lines. The multiplication amount is determined by the ratio f_1/f_2 between the two RF signals applied to the cascaded TFLN modulators. Notice that IM_1 optimizes the flatness of the comb lines with spacing f_1, while IM_2 optimizes the flatness of the comb lines with spacing f_2. The combined effect of IM_1 and IM_2 determines flatness of the final OFC [17].

In the following, we simulated the performance of the OFC by using the single-frequency-driven TFLN modulator and the dual-frequency-driven cascaded TFLN modulator schemes, respectively. According to simulated flatness results of Fig. 2, we set the parameters as $\Gamma_B = 1.4$, $\Gamma_m = 0.2$, and $\beta = 20.9$. Figure 4(a) shows the simulation results of the OFC generated by the single-frequency-driven TFLN modulator. We can see that the generated OFC has a line spacing of 25 GHz, a flatness of 3.2 dB, and 43 comb lines. By using Eq. (4), we determined the optimal parameters for flatness as $\Gamma_{m_1} = 1.7$, $\Gamma_{B_1} = 0.2$, $\Gamma_{m_2} = 2.0$, $\Gamma_{B_2} = 0.3$, and $\beta_2 = 4.6$. Based on theory and simulation, we find that the value of β_2 affects the flatness of OFC. Furthermore, when the flatness is restricted to within 10 dB, it also has an impact on the number of comb lines. To confirm that the increase in the number of comb lines scales linearly with the frequency ratio f_1/f_2 between the two RF driving signals, we set the modulation depth of $\beta_1 = 20.9$, and modulator frequencies of f_1 and f_2 to 25 GHz and 2.5 GHz, respectively. The simulation results of the OFC generated using the dual-frequency-driven cascaded TFLN modulator are shown in Fig. 4(b). We can see that the generated OFC has a line spacing of 2.5 GHz, a flatness of 10 dB, and 437 comb lines.

Experiment. To verify the proposed OFC scheme, we built two OFC systems. In the single-frequency driven TFLN modulator system, we used a 1550.12 nm continuous-wave laser with a linewidth of 100 Hz as the light source. Notice that the central wavelength of the electro-optical frequency comb is determined by that of the input laser; simply tuning the wavelength of the laser enables the EOFC to operate flexibly at different central wavelengths. A RF signal of 25 GHz, amplified by an RF amplifier, was used to drive the TFLN modulators to prepare the OFC with the simulated optimal modulation parameters. To achieve clock synchronization, the two RF sources are connected via an RF cable to share the same 10 MHz reference clock, thereby ensuring a stable phase relationship between the two RF signals. The insertion loss of the TFLN modulator is about 6 dB. In the experiment, a narrowband bandpass filter was introduced to suppress the parasitic second harmonics from the RF source and RF amplifier. A phase shifter was used to precisely control the

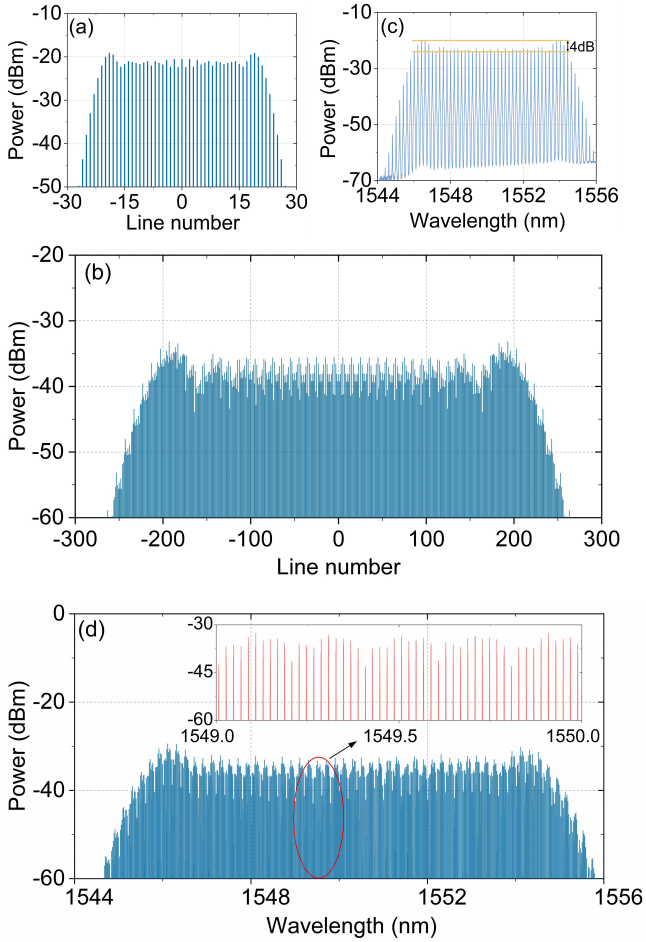

Fig. 4. (a) Simulation results of OFC generation using a single-frequency driven TFLN modulator. (b) Simulation results of OFC generation using a dual-frequency driven cascaded TFLN modulator. (c) Experimental results of OFC generation using a single-frequency driven TFLN modulator. (d) Experimental results of OFC generation using a dual-frequency driven cascaded TFLN modulator.

phase synchronization of the driving signals of the IM and PM, which is critical to improve the flatness and number of comb lines of the OFC. The prepared OFC was measured by a high-resolution optical spectrum analyzer with a precision of 0.04 pm. The measured OFC with the single-frequency driven TFLN modulators is shown in Fig. 4(c), where the generated OFC has a comb line spacing of 25 GHz, a flatness of 4 dB, and a number of comb lines of 43. The overall output power of the OFC is about −4 dBm, and the power per comb line is about −22 dBm. The experimental results are in good agreement with the simulation results.

In the dual-frequency driven TFLN modulators experiment, we used RF signals of 25 GHz and 2.5 GHz, respectively, which are amplified by RF amplifiers and then drive two cascaded TFLN modulators. In the experiment, the same modulation parameters as those in the simulations are adopted. As shown in Fig. 4(d), the prepared OFC exhibits a comb line spacing of 2.5 GHz, a flatness of 10 dB, and a total of 432 comb lines. The overall output power of the OFC is approximately −10 dBm, corresponding to about −35 dBm per comb line. The upper right corner of Fig. 4(d) shows a zoomed-in view of a portion of the

OFC spectrum. Analysis reveals that the power fluctuation of most comb lines is within 5 dB, with only about 8% of the comb lines exhibiting fluctuations around 10 dB. The number of comb lines generated by the dual-frequency-driven OFC is ten times that of the single-frequency-driven OFC, indicating that the comb line count is proportional to the frequency ratio of the two RF signals (i.e., 25/2.5 = 10). The frequency ratio between the two RF sources is the primary factor determining the comb line multiplication factor. Other factors, including the modulation depth β_2 and phase of the RF signals, also affect the multiplication factor. Notice that the electro-optic frequency response of the TFLN modulators does not affect the multiplication factor. Because both RF driving signals are single-frequency cosine signals, in this case, the modulation depth of each modulator can be separately adjusted. Experimentally, both the accuracy of phase control and clock synchronization affect the flatness of the OFC, and therefore, these parameters should be carefully tuned.

To verify the feasibility of line spacing rate tuning, we simulated the OFC characteristics of the dual-frequency-driven cascaded TFLN modulators under different frequency ratios. The frequency of the high-frequency driving signal is kept fixed, while the low-frequency driving signal is set to 1/5, 1/30, and 1/50 of the high-frequency driving signal's frequency, respectively. For frequency ratios of five, thirty, and fifty times, the generated OFC contains 225, 1327, and 2209 comb lines with flatness of 4.59 dB, 12.39 dB, and 14.47 dB, respectively. The comb line count increases proportionally with the frequency ratio. The results also indicate that the comb line spacing is determined solely by the frequency of the low-frequency driving signal. Furthermore, we experimentally measured the linewidth, phase noise, and mutual coherence of the comb lines at the spectral overlap region for the single-frequency and dual-frequency driving OFC, respectively. No evident degradation is observed, indicating that the dual-frequency driving scheme doesn't significantly compromise the system coherence.

In conclusion, we have proposed and experimentally demonstrated a simple and efficient EOFC generation scheme. By driving cascaded TFLN modulators with dual-frequency RF signals, a significant increase in the number of comb lines is achieved, which scales linearly with the frequency ratio of the two RF driving signals. Experimentally, an OFC with a line spacing of 2.5 GHz, a flatness of 10 dB, and 432 comb lines is observed. The EOFC generated using the dual-frequency-driven TFLN modulators features flexible center wavelength and line spacing, high system stability, and ease of integration. Our results overcome the limitation of the limited number of comb lines in conventional EOFCs and provide strong support for applications of EOFCs in fields such as optical communications and precision measurements.

Funding. National Natural Science Foundation of China (62205188, 62175138); Quantum Science and Technology-National Science and Technology Major Project (2021ZD0300703).

Disclosures. The authors declare no conflicts of interest.

Data availability. Datasets generated and analyzed for simulation are available from the corresponding author upon reasonable request.

REFERENCES

1. L. Lundberg, M. Mazur, A. Mirani, *et al.*, Nat. Commun. **11**, 201 (2020).
2. H. Shu, B. Shen, H. Chang, *et al.*, Photonics Insights **3**, R09 (2024).
3. Z. Wang, Y. Wang, B. Shi, *et al.*, Nat. Commun. **16**, 6853 (2025).
4. C. Qin, K. Jia, Z. Zhao, *et al.*, Optica **12**, 1747 (2025).
5. S. Bernal, M. Dumont, E. Berikaa, *et al.*, Nat. Commun. **15**, 7741 (2024).
6. T. Jiang, K. Yin, C. Wang, *et al.*, Photonics Res. **8**, 78 (2020).
7. A. Rizzo, A. Novick, V. Gopal, *et al.*, Nat. Photonics **17**, 781 (2023).
8. R. Zhuang, K. Ni, G. Wu, *et al.*, Laser Photonics Rev. **17**, 2200353 (2023).
9. I. Cardea, J. Hu, and C. -S. Bres, Opt. Express **31**, 18356 (2023).
10. C. Wang, Y. Sun, Q. Zhao, *et al.*, J. Lightwave Technol. **43**, 7650 (2025).
11. C. Chen, C. He, D. Zhu, *et al.*, Opt. Lett. **38**, 3137 (2013).
12. Q. Wang, L. Huo, Y. Xing, *et al.*, Opt. Lett. **39**, 3050 (2014).
13. C. He, S. Pan, R. Guo, *et al.*, Opt. Lett. **37**, 3834 (2012).
14. J. Wang, Q. Wang, M. Xu, *et al.*, Opt. Express **33**, 23431 (2025).
15. M. Xu, M. He, Y. Zhu, *et al.*, J. Lightwave Technol. **40**, 339 (2022).
16. Y. Dou, H. Zhang, and M. Yao, Opt. Lett. **36**, 2749 (2011).
17. V. Torres-Company, J. Lancis, and P. Andrés, Opt. Lett. **36**, 1822 (2008).